



Divergent Photoiniferter Polymerization-Induced Self-Assembly

Journal:	<i>Polymer Chemistry</i>
Manuscript ID	PY-ART-11-2024-001323.R1
Article Type:	Paper
Date Submitted by the Author:	11-Dec-2024
Complete List of Authors:	Wong, Alexander; University of Florida, Department of Chemistry Eades, Cabell; University of Florida Bowman, Jared; University of Florida, Department of Chemistry Davidson, Cullen; University of Florida Sumerlin, Brent; University of Florida, Chemistry

PAPER

Divergent Photoiniferter Polymerization-Induced Self-Assembly

Alexander J. Wong[‡], Cabell B. Eades[‡], Jared I. Bowman, Cullen L. G. Davidson IV, and Brent S. Sumerlin*

Received 00th January 20xx,
Accepted 00th January 20xx

DOI: 10.1039/x0xx00000x

Wavelength-dependent photoreactions present an opportunity to achieve chemoselectivity of functional groups that otherwise demonstrate similar reactivity under traditional thermal conditions. Relying on this concept, we demonstrate that a difunctional iniferter with two thiocarbonylthio groups can be divergently photoactivated to prepare polymeric nanoparticles via polymerization-induced self-assembly (PISA). A hydrophilic poly(oligoethylene glycol methacrylate) macroiniferter was synthesized via selective activation of one thiocarbonylthio moiety with green light. The resulting green-light-active ω -end was then further chain extended with benzyl methacrylate to obtain well-defined nanoparticles by PISA without activation of the blue-light-active α -end iniferter. The obtained nanoparticles could then be used as nanoparticle-iniferters (nanoiniferters) by chain extending from the corona with *N,N*-dimethylacrylamide via blue-light-mediated photoiniferter polymerization. This approach leverages the wavelength-dependent photolysis of thiocarbonylthio moieties to both synthesize and modify well-defined polymer nanoparticles.

Introduction

The potential of photoiniferter polymerization has experienced rapid growth in a variety of areas, including additive manufacturing,^{1,2} advanced polymer architecture development,^{3,4} and ultrahigh-molecular-weight material synthesis.^{5–7} Photoiniferter polymerization, via a mechanism similar to that of reversible addition-fragmentation chain transfer (RAFT) polymerization, imparts molecular weight control during radical polymerization via both reversible combination and degenerative chain transfer processes involving a thiocarbonylthio-based compound.⁸ However, unlike the RAFT process, in which the polymerization is initiated by the thermal decomposition of exogenous radical initiators, photoiniferter polymerizations are initiated by carbon-centered radicals produced from homolytic photolysis of the C-S bond adjacent to a thiocarbonylthio moiety.⁹ The resultant propagating radicals can then either reversibly combine with the thiocarbonylthio radical or degeneratively chain transfer to another thiocarbonylthio group. Since the amount of permanently terminated chains is proportional to the amount of exogenous initiator used in RAFT, photoiniferter polymerizations can yield polymers with higher extents of end-group retention, potentially enhancing reinitiation efficiency during subsequent chain extension.^{10,11} Efficient chain reinitiation is critical in producing well-defined block copolymer

(BCP)-based materials, such as the BCP nanoparticles obtained during polymerization-induced self-assembly (PISA).

PISA has become a powerful tool for the synthesis of polymeric nanoparticles by combining the synthesis and assembly of their constituent BCPs into one coincident process.¹¹ Most reports of PISA rely on reversible-deactivation radical polymerization (RDRP) techniques, with RAFT being the most commonly employed variant.^{12,13} Despite mechanistic similarities to RAFT PISA, photoiniferter PISA (PI PISA) remains relatively unexplored. Recently, our group, as well as the groups of Boyer and O'Reilly, have explored PI PISA technique fundamentals to prepare well-defined polymer nanoparticles.^{14–16} However, BCP nanoparticles, while chemically diverse in terms of their composition, are not generally designed with post-synthetic modification in mind. Typically, BCP nanoparticles prepared via PISA retain their reactivatable chain end within the core of the assembled particles and do not possess terminal functional groups in the coronae available for further functionalization or modification by radical chemistry. However, reports on α -end modification of BCPs in nanoparticles have been published, exploring conjugation of the nanoparticles to biological entities^{17,18} and incorporation of functional moieties such as aldehydes¹⁹ and azides^{17,20} onto the coronal chains via post-polymerization modification.

In this work, we exploit the chemoselective photosensitivity of a novel difunctional iniferter to prepare α -end functionalized polymeric nanoparticles. Similar chemoselectivity has been demonstrated in previous work by Matyjaszewski and coworkers to obtain bottlebrush and comb copolymers via

George & Josephine Butler Polymer Research Laboratory, Center for Macromolecular Science & Engineering, Department of Chemistry, University of Florida, PO Box 117200, Gainesville, Florida 32611, USA. E-mail: sumerlin@chem.ufl.edu

[‡]These authors contributed equally to this work.

*Electronic Supplementary Information available. See DOI: 10.1039/x0xx00000x

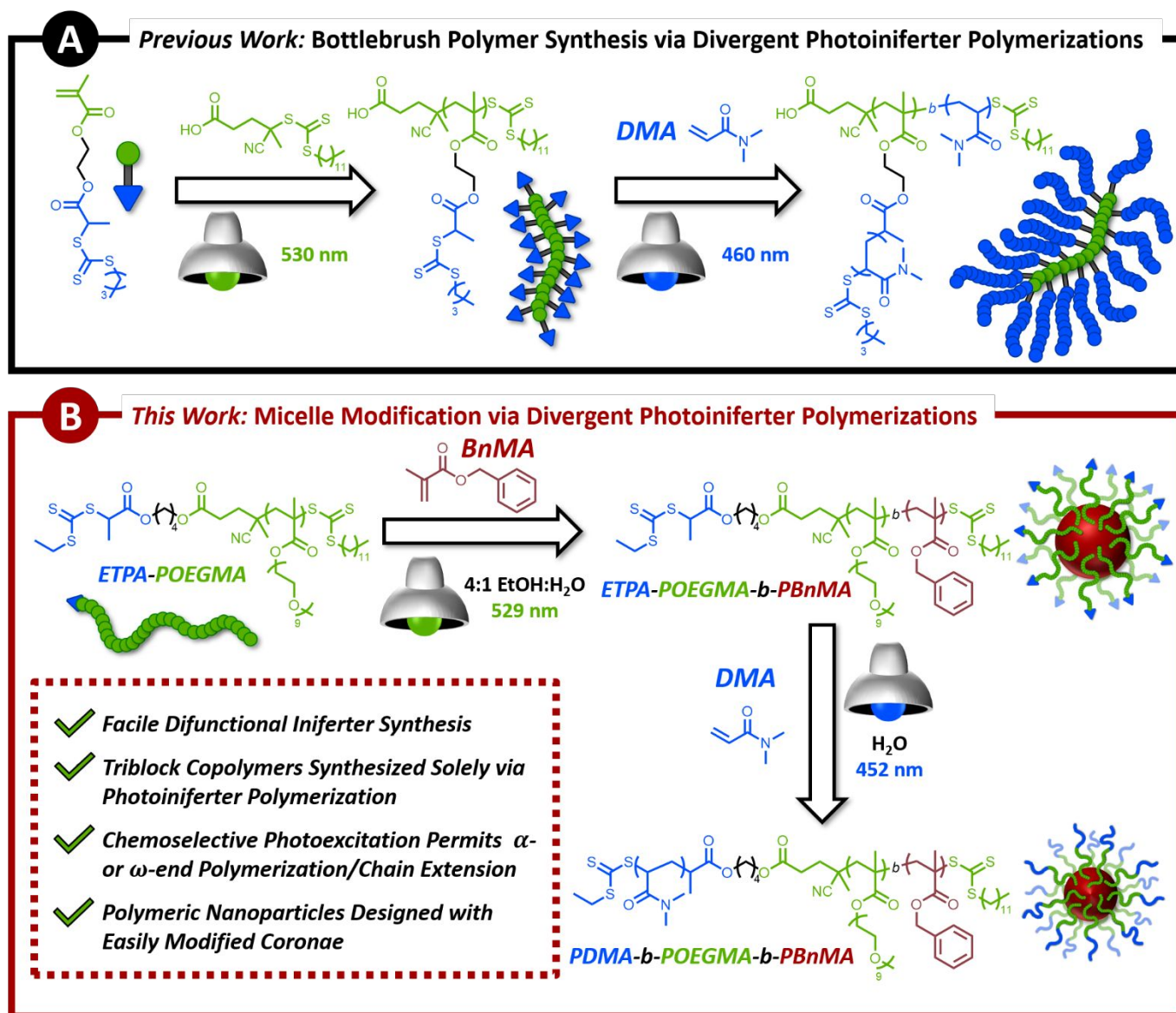


Fig. 1 (A) Previous work, wherein a methacrylate-functionalized blue-light-active iniferter (far left) is polymerized via green-light-mediated photoiniferter polymerization using a green-light-active iniferter to yield a polymethacrylate bearing pendent blue-light-active trithiocarbonates on each repeat unit (center). *N,N*-Dimethylacrylamide (DMA) was polymerized via blue-light-mediated photoiniferter polymerization from the pendent trithiocarbonate moieties as well as the backbone ω -end to yield bottlebrush polymers.³ (B) This work, wherein blue-light- and green-light-active trithiocarbonates were coupled to yield a difunctional iniferter that could be activated at one end with blue light and the other end with green light. Under green light, a poly(oligoethylene glycol methacrylate) (POEGMA) macroiniferter was synthesized. Green-light-mediated photoiniferter polymerization-induced self-assembly (PI PISA) was then carried out with benzyl methacrylate (BnMA), giving POEGMA-*b*-PBnMA nanoparticles with α -end trithiocarbonate-functionalized coronal chains. DMA could then be polymerized from the α -end iniferters without also adding to the ω -ends sequestered in the nanoparticle cores.

difunctional iniferter reported here features two distinct thiocarbonylthio moieties selected such that only one is sensitive to green light irradiation. This selectivity enabled us to employ green-light-mediated PI PISA for the preparation of poly(oligoethylene glycol methacrylate)-*b*-poly(benzyl methacrylate) (POEGMA-*b*-PBnMA) nanoparticles that bear unreacted blue-light-sensitive iniferters on the outside peripheries of the coronae. Subsequent irradiation with blue light allowed chemoselective chain extension from the α -termini of the BCPs in the nanoparticle coronae with *N,N*-dimethylacrylamide (DMA) without monomer addition to the ω -termini sequestered in the hydrophobic nanoparticle cores

(Figure 1B). These divergent photochemical pathways used to obtain highly tunable polymeric nanostructures could provide possible new pathways for the synthesis and modification of polymeric nanomaterials made via photoiniferter polymerization.

Results and discussion

Difunctional iniferter synthesis

To start, we selected two iniferters that absorb distinct wavelengths of visible light to achieve chemoselective photoactivation. Inspired by the work of Matyjaszewski and coworkers (Figure 1A),³ we chose 4-cyano-4-

((dodecylthio)carbonothioyl)thio)pentanoate (CDP) (blue- and green-light-active) and 2-((ethylthio)carbonothioyl)thio)propionate (ETPA) (green-light-inactive but blue-light-active). UV-vis spectroscopy was used to measure the excitation wavelengths for these iniferters (Figure 2B). With confirmation that ETPA did not absorb green light (529 nm), while CDP did, we then synthesized a difunctional iniferter via consecutive Steglich esterification reactions of ETPA and CDP to 1,4-butanediol (Figure 2A). This compound was characterized using ^1H NMR spectroscopy (Figures S1-4) and mass spectrometry (MS) (Figures S7-9).

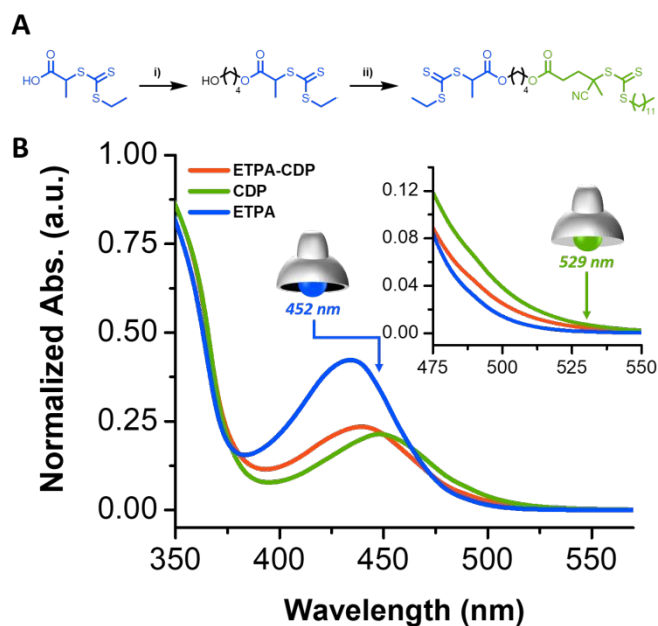


Fig. 2 (A) Reaction scheme of the difunctional iniferter synthesis. Reaction conditions: (i) 1-ethyl-3-(3-dimethylaminopropyl)carbodiimide (EDC), 4-dimethylaminopyridine (DMAP_{cat}), 1,4-butanediol, dichloromethane (DCM), 6 h, 0 °C to rt. (ii) 4-cyano-4-((dodecylthio)carbonothioyl)thio)pentanoate (CDP), EDC, DMAP_{cat} , DCM, 12 h, 0 °C to rt. (B) UV-vis absorption spectra of CDP (green), 2-((ethylthio)carbonothioyl)thio)propionate (ETPA, blue) and the ETPA-CDP difunctional iniferter (orange). Inset plot shows the negligible sensitivity of ETPA to green light.

Macroiniferter synthesis

Using ETPA-CDP, oligoethylene glycol methacrylate (OEGMA, $M_n = 500$) was polymerized via green-light-mediated photoiniferter polymerization (529 nm, 100 mW/cm^2), yielding a poly(OEGMA) (POEGMA) macroiniferter (Figure 3A). Under green light, the CDP end of the iniferter is selectively photolyzed and chain transfer of the propagating methacryloyl chain end to the ETPA is expected to be unfavorable, according to previous reports.^{3,21} A monomodal shift to lower elution times (Figure 3B), linear pseudo-first-order kinetics (Figure S10), and good agreement between theoretical and experimental molecular weights were observed (Figure 3C), all consistent with a well-controlled polymerization ($M_{n,\text{Theo}} = 20.9$ kg/mol, $M_{n,\text{SEC}} = 20.3$ kg/mol, $\mathcal{D} = 1.14$). The ^1H NMR spectrum of the macroiniferter showed negligible change in the chemical shift of the methine proton ($\delta = 4.81$ ppm) of the ETPA moiety, indicating that the

blue-light active trithiocarbonate largely remained inactive during polymerization (Figure 3D).

Control experiments were performed to further demonstrate the divergent activation of the difunctional iniferter. When a solution of ETPA and OEGMA in 1,4-dioxane was irradiated with green light (529 nm, 100 mW/cm^2), SEC analysis indicated no POEGMA formation (Figure S13), confirming the insensitivity of the ETPA moiety to green light as suggested by UV-vis spectroscopy (Scheme S1A). Subsequently, a solution of OEGMA (45 equiv) with CDP (1.0 equiv) and ETPA (1.0 equiv) in 1,4-dioxane was exposed to the same green light conditions (Scheme S1B). We hypothesized that if chain transfer between CDP and ETPA were to occur, the molecular weight of the resultant POEGMA would be half that of POEGMA synthesized only with 1.0 equiv of CDP (Scheme S1C). However, these two polymerizations yielded POEGMA of near-identical molecular weights, indicating no significant chain transfer of the propagating methacryloyl chain end to the ETPA group under green light conditions. Furthermore, the SEC traces of the resultant POEGMA overlap with that of POEGMA synthesized with the ETPA-CDP difunctional iniferter (Figure S13). Based on our findings from these control experiments and previous literature precedents, we concluded that the ETPA moiety is insensitive to green-light-activation and does not participate in

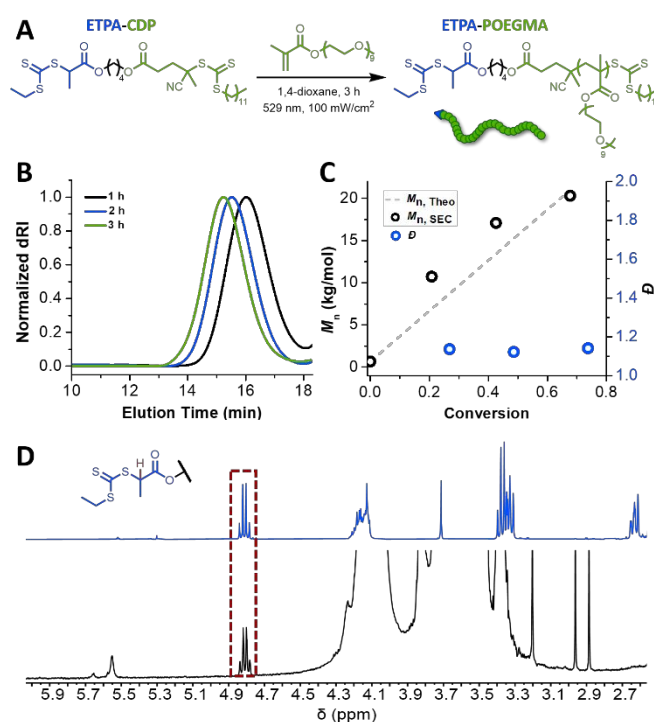


Fig. 3 (A) Reaction scheme showing the synthesis of ETPA α -end functionalized POEGMA (ETPA-POEGMA) (B) Size exclusion chromatography (SEC) elugrams taken during POEGMA synthesis, showing monomodal shifts toward lower elution times indicative of increasing molecular weight. (C) $M_{n,\text{SEC}}$ versus monomer conversion, showing close agreement with $M_{n,\text{Theo}}$ while maintaining low dispersities (\mathcal{D}). (D) ^1H NMR spectra of ETPA-CDP (top, blue) and ETPA-POEGMA (bottom, black) highlighting no change in the chemical shift of the methine proton (red, $\delta = 4.81$ ppm) on ETPA during POEGMA synthesis, suggesting OEGMA polymerization predominantly occurred via photoactivated homolysis of the CDP moiety.

degenerative transfer during OEGMA polymerization. After confirming the divergent nature of the difunctional iniferter reactivity, we then sought to synthesize polymeric nanoparticles via photoiniferter polymerization-induced self-assembly (PI PISA).

Photoiniferter polymerization-induced self-assembly (PI PISA)

PI PISA reactions were then performed by chain extending the ETPA-POEGMA macroiniferter with benzyl methacrylate (BnMA) under green light irradiation (529 nm, 100 mW/cm²) in 4:1 EtOH:H₂O (w/w) as the solvent at 20% w/w solids (Figure 4A). An ethanol/water solvent mixture was chosen to favor the formation of kinetically trapped micelles that simplified subsequent coronal chain extension and analysis. A core number-average degree of polymerization (DP) of 200 was targeted in order to further ensure spherical micelles were obtained. SEC analysis revealed a monomodal increase in molecular weight with minimal tailing observed, indicating high maintenance of ω -end fidelity (Figure 4B). Kinetic analysis of the polymerization revealed a significant increase in the apparent propagation rate constant ($k_{p,app}$) after self-assembly was qualitatively observed (the solutions transitioned from

transparent and yellow before self-assembly to translucent/opaque-white, free-flowing dispersions of nanoparticles), an observation consistent with typical PISA kinetics (Figure 4C).^{22,23} As the nanoparticles became larger and the reaction solution became more turbid, a tapering of $k_{p,app}$ was observed, an observation we attribute to higher light attenuation resulting from solution opacity increasing. Dynamic light scattering (DLS) analysis of the resultant nanoparticles yielded a Z-average hydrodynamic diameter (D_h) of 81 nm with a narrow polydispersity index (PDI = 0.085) (Figure 4D). Transmission electron microscopy (TEM) was used to discern nanoparticle morphology. To prevent nanoparticle dissociation during TEM sample preparation, crosslinked nanoparticles were synthesized with 1 mol% ethylene glycol dimethacrylate (EGDMA) in the core. Upon TEM image analysis, we observed distinct spherical morphologies (Figure 4E).

Coronal chain extension

Once successful ETPA-POEGMA-*b*-PBnMA nanoparticle synthesis was confirmed, we then sought to chain extend from the ETPA iniferter located at the α -end of the unimer chains. A 20% w/w solution of ETPA-POEGMA-*b*-PBnMA nanoparticle-iniferters (nanoiniferters) was diluted with water and allowed to equilibrate, after which a 2 M solution of *N,N*-dimethylacrylamide (DMA) in water was added. DLS measurements showed no appreciable size change after dilution and addition of DMA, suggesting that DMA did not appreciably swell the nanoparticle cores (Figure S14). Coronal chain extension was then carried out via blue-light-mediated photoiniferter polymerization (452 nm, 8.5 mW/cm²) exclusively at the α -end ETPA iniferter (Figure 5A). After 12 h of irradiation, approximately 25% of the DMA had been polymerized, forming a new poly(*N,N*-dimethylacrylamide) (PDMA) block extending from the peripheries of the nanoiniferter coronae. SEC analysis of the resultant PDMA-*b*-POEGMA-*b*-PBnMA revealed a clean shift to higher elution times with no increase in tailing compared to ETPA-POEGMA and ETPA-POEGMA-*b*-PBnMA, indicative of high α -end fidelity (Figure 5B). A Z-average D_h of 237 nm was measured via DLS for the nanoparticles chain extended from their coronae (Figure 5C). TEM imaging of the nanoparticles that had been core-crosslinked with EGDMA (1 mol%) showed little difference in size before and after coronal extension; we attribute this observation to the majority of contrast in the micrograph arising from the nanoparticle core, which remained unchanged by the chain extension. (Figure 5D).

To further elucidate the unique ability of ETPA-CDP to allow α -end chain extension from the nanoiniferter coronae, we performed control experiments using two molecules of CDP tethered by 1,4-butanediol (diCDP) (Figures S5, S6). Macroiniferter and nanoparticle syntheses were carried out under identical conditions to those used to prepare ETPA-POEGMA and ETPA-POEGMA-*b*-PBnMA, respectively. We reasoned that the difunctional and symmetrical nature of diCDP would result in a telechelic POEGMA macroiniferter, and that chain extension with BnMA from both ends would yield PBnMA-*b*-POEGMA-*b*-PBnMA BAB triblock copolymers (Scheme S2).

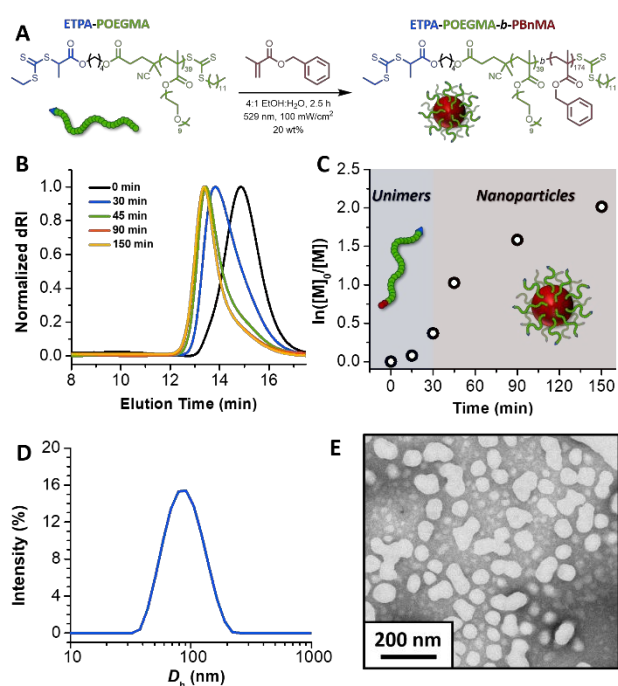


Fig. 4 (A) Reaction scheme of the photoiniferter polymerization-induced self-assembly (PI PISA) of ETPA-POEGMA with benzyl methacrylate (BnMA) under green-light irradiation in 4:1 EtOH:H₂O (w/w). (B) SEC elugrams of kinetic timepoints taking during the polymerization showing monomodal shifts to shorter elution times indicative of increasing molecular weights of the ETPA-POEGMA-*b*-poly(BnMA) (ETPA-POEGMA-*b*-PBnMA) chains. (C) Pseudo-first-order kinetic plot of the PISA reaction showing an increase in $k_{p,app}$ from before (blue region, $k_{p,app} = 8.61 \times 10^{-5} \text{ s}^{-1}$) and after (red region, $7.29 \times 10^{-4} \text{ s}^{-1}$) self-assembly was qualitatively observed. (D) Dynamic light scattering (DLS) trace of ETPA-POEGMA-*b*-PBnMA nanoparticles crosslinked with ethylene glycol dimethacrylate (EGDMA, 1 mol%) in 4:1 EtOH:H₂O (0.1 w/w%) (Z-average hydrodynamic diameter (D_h) = 81 nm, PDI = 0.085) (E) Transmission electron microscopy (TEM) image of ETPA-POEGMA-*b*-P(BnMA-co-EGDMA) nanoparticles.

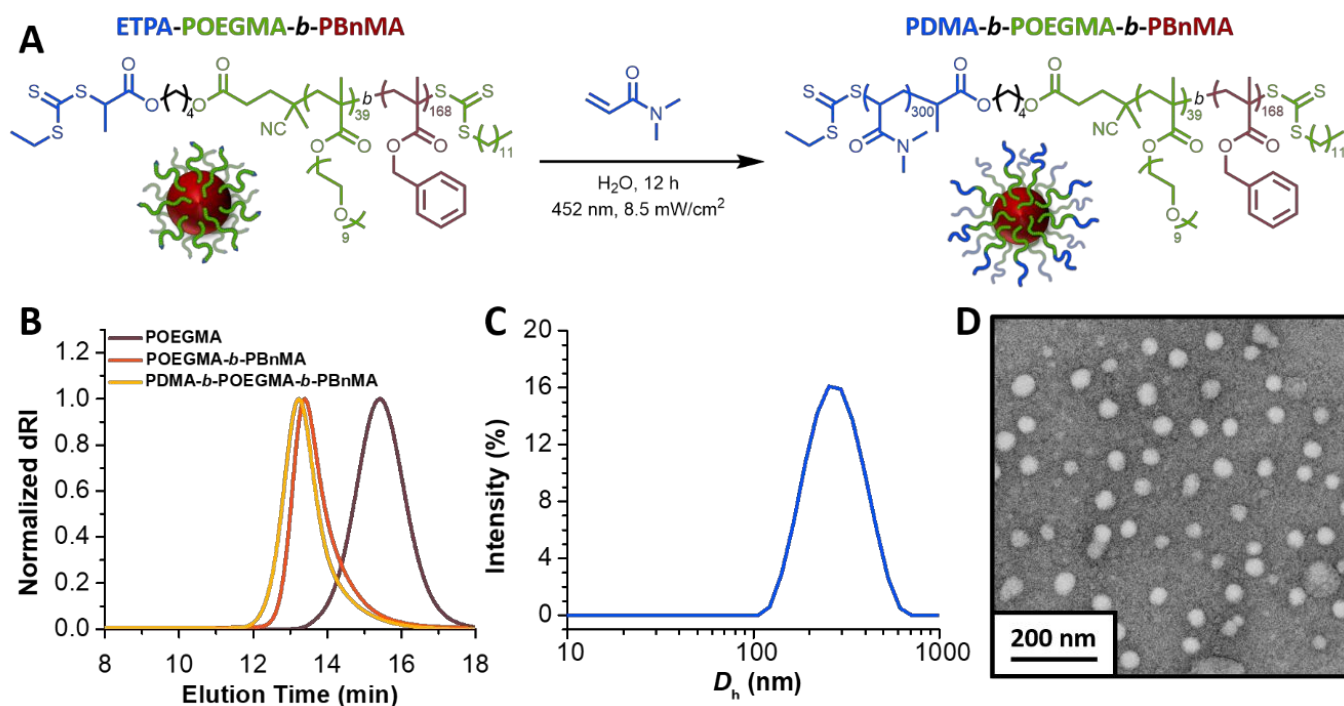


Fig. 5 (A) Reaction scheme for the chain extension from the blue-light-active α -end of ETPA-POEGMA-*b*-PBnMA nanoiniferter unimers. (B) SEC elugrams of ETPA-POEGMA (red), ETPA-POEGMA-*b*-PBnMA (orange), and PDMA-*b*-POEGMA-*b*-PBnMA (yellow), showing a progression to shorter elution times indicative of an increasing molecular weight with each chain extension. (C) DLS trace of PDMA-*b*-POEGMA-*b*-PBnMA nanoparticles in 4:1 EtOH:H₂O (0.1 w/w%) crosslinked with EGDMA (1 mol%) (Z-average D_h = 327 nm, PDI = 0.192). (D) TEM image of PDMA-*b*-POEGMA-*b*-P(BnMA-co-EGDMA) nanoparticles.

This block sequence should yield flower-like nanoparticles with both terminal thiocarbonylthio moieties sequestered in the PBnMA core, making coronal chain extension with DMA impossible.^{24,25} Upon exposure to blue light in the presence of DMA, the chains comprising the PBnMA-*b*-POEGMA-*b*-PBnMA nanoparticles did not chain extend, as confirmed by SEC analysis (Figure S13). Instead, the SEC elugram showed a high molecular weight shoulder adjacent to the larger PBnMA-*b*-POEGMA-*b*-PBnMA peak, which we attributed to chain coupling in the core induced by blue light activation of the thiocarbonylthio moieties located there in the absence of monomer. These model experiments are consistent with the divergent chain extension of the core and corona trithiocarbonates under the conditions employed.

Conclusions

These results demonstrate the potential of exploiting chemoselectivity via wavelength-dependent photoreactions to enable chain extension from two functional groups that otherwise demonstrate similar reactivity under traditional thermal conditions. Our findings show that a difunctional iniferter with two thiocarbonylthio groups can be divergently photoactivated to prepare complex polymeric nanoparticles by exploiting the self-assembly and selective solubility quintessential to the PISA process. This approach leverages the wavelength-dependent photolysis of thiocarbonylthio moieties to both synthesize and modify well-defined polymer nanoparticles and suggests that divergent photoiniferter

polymerizations may provide new avenues for development of functional and precisely customizable polymeric nanomaterials.

Conflicts of interest

There are no conflicts to declare.

Data availability

The data supporting this article have been included as part of the Supplementary Information.

Acknowledgements

This material is based on work supported by the National Science Foundation (DMR-2404144) and DoD through the ARO (W911NF2410050).

Notes and references

- 1 A. Bagheri and J. Jin, *Polym. Chem.*, 2020, 11, 641-647.
- 2 B. Zhao, J. Li, Y. Xiu, X. Pan, Z. Zhang and J. Zhu, *Macromolecules*, 2024, 21, 1620-1628.

- 3 S. Shanmugam, J. Cuthbert, T. Kowalewski, C. Boyer and K. Matyjaszewski, *Macromolecules*, 2018, 51, 7776–7784.
- 4 S. Allison-Logan, F. Karimi, Y. Sun, T. G. McKenzie, M. D. Nothling, G. Bryant and G. G. Qiao, *ACS Macro Lett.*, 2019, 8, 1291–1295.
- 5 M. E. Lott, L. Trachsel, E. Schué, C. L. G. Davidson, R. A. Olson S, D. I. Pedro, F. Chang, Y. Hong, W. G. Sawyer and B. S. Sumerlin, *Macromolecules*, 2024, 57, 4007–4015.
- 6 R. N. Carmean, T. E. Becker, M. B. Sims and B. S. Sumerlin, *Chem*, 2017, 2, 93–101.
- 7 R. N. Carmean, M. B. Sims, C. A. Figg, P. J. Hurst, J. P. Patterson and B. S. Sumerlin, *ACS Macro Lett.*, 2020, 9, 613–618.
- 8 M. Hartlieb, *Macromol. Rapid Commun.*, 2022, 43, 2100514.
- 9 R. W. Hughes, M. E. Lott, J. I. Bowman and B. S. Sumerlin, *ACS Macro Lett.*, 2023, 12, 14–19.
- 10 A. C. Lehnen, J. A. M. Kurki and M. Hartlieb, *Polym. Chem.*, 2022, 13, 1537–1546.
- 11 N. J. W. Penfold, J. Yeow, C. Boyer and S. P. Armes, *ACS Macro Lett.*, 2019, 23, 1029–1054.
- 12 N. J. Warren and S. P. Armes, *J. Am. Chem. Soc.*, 2014, 136, 10174–10185.
- 13 S. L. Canning, G. N. Smith and S. P. Armes, *Macromolecules*, 2016, 49, 1985–2001.
- 14 J. I. Bowman, C. B. Eades, M. A. Vratsanos, N. C. Gianneschi and B. S. Sumerlin, *Angew. Chem. Int. Ed.*, 2023, 62, e202309951.
- 15 J. Yeow, O. R. Sugita and C. Boyer, *ACS Macro Lett.*, 2016, 5, 558–564.
- 16 L. D. Blackman, K. E. B. Doncom, M. I. Gibson and R. K. O'Reilly, *Polym. Chem.*, 2017, 8, 2860.
- 17 A. B. Korpusik, Y. Tan, J. B. Garrison, W. Tan and B. S. Sumerlin, *Macromolecules*, 2021, 54, 7354–7363.
- 18 T. Lückerrath, K. Koynov, S. Loescher, C. J. Whitfield, L. Nuhn, A. Walther, C. Barner-Kowollik, D. Y. W. Ng and T. Weil, *Angew. Chem. Int. Ed.*, 2020, 59, 15474–15479.
- 19 E. C. Johnson, S. Varlas, O. Norvilaite, T. J. Neal, E. E. Brotherton, G. Sanderson, G. J. Leggett and S. P. Armes, *Chem. Mat.*, 2023, 35, 6109–6122.
- 20 I. Akar, A. K. Pearce, C. M. S. Kumar, C. Ferguson and R. K. O'Reilly, *J. Polym. Sci.*, 2023, 61, 2932–2944.
- 21 S. Yang, L. Zhang, Y. Chen and J. Tan, *Macromolecules*, 2022, 55, 8472–8484.
- 22 J. I. Bowman, C. B. Eades, J. Korpanty, J. B. Garrison, G. M. Scheutz, S. L. Goodrich, N. C. Gianneschi and B. S. Sumerlin, *Macromolecules*, 2023, 56, 3316–3323.
- 23 G. M. Scheutz, J. I. Bowman, S. Mondal, J. Y. Rho, J. B. Garrison, J. Korpanty, N. C. Gianneschi and B. S. Sumerlin, *ACS Macro Lett.*, 2023, 12, 454–461.
- 24 P. Biais, O. Colombani, L. Bouteiller, F. Stoffelbach and J. Rieger, *Polym. Chem.*, 2020, 11, 4568–4578.
- 25 Y. Mizoue, E. Onodera, K. Haraguchi and S. I. Yusa, *Polymers*, 2022, 14, 1678.

Data availability

The data supporting this article have been included as part of the Supplementary Information.